Photoconductance Determination of Carrier Capture Cross Sections of Slow Traps in Silicon Through Variable Pulse Filling

Manjula Siriwardhana, Yan Zhu, Ziv Hameiri, Daniel Macdonald, and Fiacre Rougieux

***Abstract*—The capture cross sections are a key metric to characterize carrier traps in semiconductors. In this article, photoconductance measurements are used to estimate the capture cross sections of traps that are induced by thermal donors in Czochralski-grown silicon wafers. Here, we use a pulse-filling technique with light-emitting diode excitation to measure the capture rate. The measured capture rates are shown to be similar to the values that were measured previously by deep-level transient spectroscopy. Our method allows the contactless measurements of the capture cross sections. The minority carrier cross sections for the two distinct trap states that are studied here are of the order of 10^{-18} cm^2 and the majority carrier cross sections are orders of magnitude smaller. Therefore, it is concluded that the slow traps that are originating from the thermal donors are dominated by the minority carrier trapping.**

***Index Terms*—Carrier traps, capture cross section, lifetime measurement, silicon, thermal donors.**

I. Introduction

INJECTION-dependent carrier lifetimes that are obtained via quasi-steady-state or transient photoconductance measurements are commonly used in silicon photovoltaics research [1]. However, these measurements are sometimes affected by artifacts that are arising from trapping centers [2]. In photoconductance-based measurements, such traps can lead to a sharp increase in the apparent lifetime at low injection levels [3]. These traps do not necessarily contribute to recombination and interact mainly with minority carriers [3]. Such trapping centers can be considered to be "fast" traps, as they have capture and emission time constants shorter than the recombination lifetime. Similarly, the "slow" traps interact with minority carriers and release carriers back into the bands, but, at a rate much lower than the recombination lifetime. Such slow traps have been observed in Czochralski (Cz) silicon samples [4]–[9]. Understanding slow trapping of minority carriers is important in the characterization of silicon materials for photovoltaics. For example, studying oxygen-related trapping will help to understand the properties of thermal donors. Several methods, such as quasi-steady-state photoconductance (QSSPC) [10], photoconductance decay [11], and microwave detected photoconductance decay [12], [13], have been used to study fast and slow trapping effects in silicon materials.

Thermal donors are caused by clusters of oxygen impurities with different atomic configurations [14], [15]. The concentration of each configuration is determined by the annealing time and temperature [15], usually between 350 and 500 °C. Thermal donors are correlated with a significant loss of efficiency in silicon heterojunction solar cells [16], [17]. These thermal donors also introduce slow traps in Cz-grown silicon wafers [7], [8]; and high concentrations of thermal donors lead to more than one species of slow trap [7], [8]. As such, it is important to understand the recombination and trapping properties of thermal donors.

Previous studies have focused on the recombination parameters of thermal donors [17], their temperature dependence [18], and the emission properties of thermal-donor-related traps (detrapping time constants and energy levels) [7], [19]. However, little is known regarding the capture parameters of thermal donors and their dependence on temperature.

Many methods to identify defects levels and their capture rates and capture cross sections, such as deep level transient spectroscopy (DLTS) [20], [21], Laplace DLTS [22], and thermally stimulated current (TSC) [23], have been developed over the years. However, some of these methods are limited in their use. For example, DLTS requires low concentrations of background doping and only detects defects in the depletion region near the surface, while TSC requires low dark currents to obtain accurate measurements of defects [24]. These methods are also limited in their sensitivity to deep defects [24]. Additionally, methods such as DLTS and TSC are destructive and require considerable effort in sample preparation. On the other hand, photoconductance measurements can be applied with a minimal

Manuscript received October 17, 2020; revised November 24, 2020; accepted December 2, 2020. Date of publication January 11, 2021; date of current version February 19, 2021. This work was supported in part by the Australian Research Council under Project DE160101368 and in part by the Australian Renewable Energy Agency (ARENA Projects RND001 and RND017). The work of Yan Zhu was supported by the fellowship by the Australian Centre for Advanced Photovoltaics (ACAP, Project RG200768-G). *(Corresponding author: Manjula Siriwardhana.)*

Manjula Siriwardhana and Daniel Macdonald are with the Research School of Electrical, Energy and Materials Engineering, The Australian National University, Canberra, ACT 2601, Australia (e-mail: mtsiriwardhana@gmail.com; daniel.macdonald@anu.edu.au).

Yan Zhu, Ziv Hameiri, and Fiacre Rougieux are with the School of Photovoltaic and Renewable Energy Engineering, University of New South Wales, Sydney, NSW 2052, Australia (e-mail: yan.zhu@unsw.edu.au; z.hameiri@unsw.edu.au; fiacre.rougieux@unsw.edu.au).

Color versions of one or more of the figures in this article are available online at https://doi.org/10.1109/JPHOTOV.2020.3043835.

Digital Object Identifier 10.1109/JPHOTOV.2020.3043835

sample preparation. These measurements are sensitive to defects throughout the silicon bulk.

The variable pulse-filling technique is commonly used to estimate the capture cross section of deep impurity levels in transient spectroscopy applications [20], [25], [26]. The change in trap filling is typically measured via the change in the dark capacitance [25], [26], photocapacitance [26]–[28], or the current [20] of a Schottky diode as a function of filling pulsewidth. Such studies have focused mainly on deep-level metal impurities [4], [21], [28] and fast traps that require a pulsewidth in the microsecond range [21]. More recently, the pulse-filling technique was also used to study multiple deep levels that are induced by thermal donors in Cz silicon materials via DLTS techniques [7].

In this study, we present a new nondestructive method to measure the capture cross sections of slow traps caused by thermal donors using the transient photoconductance decay combined with a variable pulse-filling method. Here, a simplified analysis of trap filling kinetics is used to obtain the capture rate of holes, c_p. This technique also allows discriminating between several traps with similar filling rates. The main advantage of this technique over more traditional capacitance transient techniques is that it is simple and contactless. In principle, the method is applicable to a wide range of substrates with limitations imposed mainly by the available transient electrical properties of the light source (such as the shortest light illumination time).

II. Theory and Background

In this section, we outline the principle of the proposed method. For this analysis, we assume a deep minority carrier trap in an n-type silicon wafer. The trap concentration is N_T and has an initial thermal occupancy of minority carriers (holes in this case) $p_T(0)$. At any given time t, p_T is the concentration of traps occupied by holes, thus, p_T states are able to emit holes or capture electrons and $(N_T - p_T)$ states are able to capture holes and emit electrons.

The occupancy of a state is determined by the competing emission and capture processes. Assuming that the traps interact with both the valence band and the conductance band, the net rate of change of holes is given by

$$\frac{dp_T}{dt} = (c_p + e_n) \times (N_T - p_T) - ((e_p + c_n) \times p_T) \quad (1)$$

where

e_p = emission rate of holes;
c_p = capture rate of holes;
e_n = emission rate of electrons; and
c_n = capture rate of electrons.

At $t = \infty$

$$p_T(\infty) = N_T \times \frac{c_p + e_n}{c_p + e_n + e_p + c_n}. \quad (2)$$

On the assumption that total trap concentration N_T is much smaller than the doping n_0 ($N_T << n_0$) and the sample is subjected to low injection, where the excess carrier generation

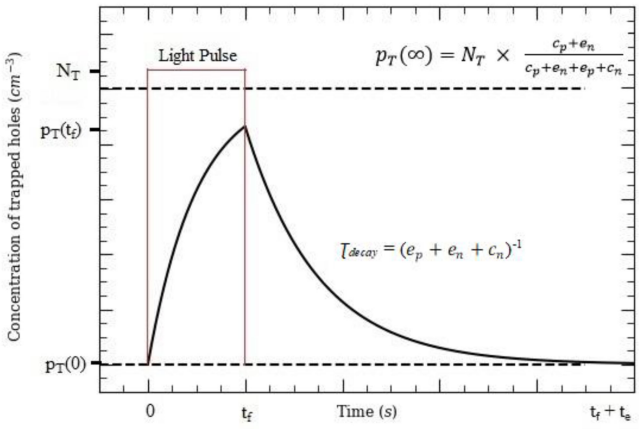

Fig. 1. Concentration of trapped holes as a function of time. While the LED pulse is ON, the concentration of trapped holes rises and they are subsequently emitted when the filling pulse is turned OFF.

Δn and Δp are much smaller than the doping, n_0 (Δn, $\Delta p << n_0$), during the filling pulse, the concentration of traps occupied by holes varies according to (3) [29]. Here, if the trap concentration is much higher than the dopant concentration, the density of free carriers available for capture will decay with time.

$$p_T(t) - p_T(0) = \{p_T(\infty) - p_T(0)\} \times \{1 - \exp[-(e_p + c_p + e_n + c_n)\, t]\}. \quad (3)$$

Hence, the time constant of the trap filling process is given by

$$\tau_{\text{fill}} = (e_p + c_p + e_n + c_n)^{-1}$$

For transient photoconductance decay measurements, if the recapture of minority carriers by the trap is negligible (the validity of this assumption will be discussed later), the PC decay due to a single-level trap is an exponential decay with a time constant [11]

$$\tau_{\text{decay}} = (e_p + e_n + c_n)^{-1}. \quad (4)$$

In the presence of slow traps, after a sample is illuminated with a light source and the light is terminated, there is a long slow decay of photoconductance as represented schematically in Fig. 1. The filling of all the traps typically occurs in a matter of microseconds and the emission occurs over a much slower phase. Note that the rise of the photoconductance during filling is also impacted by the conductance due to free carriers in the bands. It is often challenging to distinguish between recombination active carriers and extra charge due to trapping, whereas during the emission, the decay due to detrapping is much slower than the decay due to recombination of carriers in the band. Therefore, it is more accurate to distinguish the photoconductance decay due to recombination active defects and trapping from the decay curve than from the filling curve.

Therefore, a method of using the transient decay instead of the filling transient to measure the capture rate was suggested [29]. The key is to examine the emission transient for varying pulse-filling times. Since the decay rates can be much slower than the filling rates and a considerable difference between the decay

rates of the two traps often exists, much longer pulse times can be used to calculate the filling rates. The different components of the emission transient allow resolving the different traps that have been filled during the filling pulse. A key point is that the filled trap concentration at the end of filling time, t_f is equal to the concentration of filled traps at the beginning of the decay curve.

At the end of filling pulse time t_f, the concentration of filled minority carrier traps is given by (3).

The fraction of minority carrier traps that are not yet filled at the time t_f, $F_T(t_f)$, is

$$F_T(t_f) = 1 - \frac{p_T(t_f) - p_T(0)}{p_T(\infty) - p_T(0)}. \tag{5}$$

From (2), (3), and (5)

$$F_T(t_f) = \exp\left[-\left(c_p + e_n + c_n + e_p\right) t_f\right]. \tag{6}$$

Fitting the emission transient allows the decay rate, $(e_n + c_n + e_p)^{-1}$, to be obtained. Fitting (6) to the measured hole trap concentration allows the extraction of the decay and filling rates. Combining these two results allows the determination of the hole capture rate c_p.

Using the change in conductance (calculated from the change in voltage at each pulse filling), the filled concentration is determined. Then, $F_T(t_f)$ at each pulse filling length is calculated. Note that conversion from photoconductance to excess carrier density requires knowledge of the hole mobility. Here, the model of Arora *et al.* [30] is used to calculate the hole mobility of the sample. It is suitable for the modeling of low injection lifetime and conductance measurements since it includes temperature and dopant density dependencies, but not the impact of carrier–carrier scattering.

The majority carrier capture rate, c_n, is dependent on the dopant density at a low injection level

$$c_n = \sigma_n \times v_n \times n_0 \tag{7}$$

where is v_n thermal velocity of electrons and n_0 is the dopant concentration. By plotting $1/\tau_{\mathrm{decay}}$ versus n_0, the majority carrier capture cross section can be determined [11]

$$1/\tau decay = \sigma_n \times (v_n \times n_0) + (e_n + e_p). \tag{8}$$

As shown in Fig. 1, when the light-emitting-diode (LED) light is ON, the occupancy of the states are determined according to (1) and if the filling time is long enough to reach the steady-state occupancy level that is shown as $p_T(\infty)$, the conductance remains unchanged as long as the light is ON. Once the light is OFF, after the recombination decay, the slow traps start decaying as a rate given by (8) until the conductance value reaches the dark conductance.

III. Experimental Methods

In this study, four sister wafers from an n-type monocrystalline Cz silicon ingot with as-cut resistivity of 1.1 Ω.cm were used. The samples were first annealed at 650 °C for 30 min to remove any preexisting thermal donors. One sample was kept as a control and the remaining samples were annealed at 450 °C for 72 h, 96 h, and 144 h to create a range of thermal donor concentrations. All samples were then RCA cleaned and passivated with silicon nitride (SiN_x) using plasma-enhanced chemical vapor deposition (PECVD) on both surfaces. The resistivity and thermal donor concentrations were determined via the dark conductance measured with a WCT-120 system from Sinton Instruments [31]. After thermal donor generation, the resistivity of the samples ranged from 1.1 Ω.cm (nonannealed sample) to 0.3 Ω.cm (144 h annealed sample). The thermal donor concentration within each sample was determined by the change in dopant density (determined from the change in resistivity) and considering the fact that thermal donors are double donors.

Photoconductance decay measurements were carried out using a modified WCT-120 lifetime tester [32] where the conductance of a sample is measured with an inductively coupled coil. The system includes an additional photoluminescence (PL) sensor, in addition to the photoconductance coil. The system also includes an additional LED with a wavelength of 810 nm as a light source, in addition to the xenon flash with a decay time constant of 2.3 ms that is used in the standard WCT-120 tools. The LED allows steady-state excitation at various intensities. The setup is placed in a light-tight box to eliminate the background light. In this study, the samples were kept in the dark for at least 10 min before each measurement to ensure that the trap occupancy is at thermal equilibrium.

The injection-dependent carrier lifetime was initially measured using the QSSPC and quasi-steady-state photoluminescence (QSSPL) techniques [3]. Minority carrier trapping was identified from the artificially high lifetime at low injection levels. All the samples were then tested for changes in their transient photoconductance during a slow detrapping process at two different temperatures (30 and 55 °C).

In order to analyze the emission (or detrapping) process, the samples were illuminated with a flash and the decay of the photoconductance voltage was measured for 10 min after its termination. Here, in order to analyze whether there is any impact of the level of excitation or the source of light on the decay time constants, a flash illumination is used. The sample without thermal donors (control sample) did not show an extended slow decay of the photoconductance [4], [19], [33]. As shown in Fig. 2, the samples with thermal donors showed a pronounced extended photoconductance decay (which is much longer than the minority carrier lifetime of the sample, 40 μs in this case). This pronounced photoconductance decay is associated with the detrapping of minority carriers from the traps [4], [8]. The fact that the detrapping time constant is much longer than the minority carrier lifetime provides a good support for the assumption of (8). Since two exponential curves are required to fit the photoconductance decay, it seems there are two distinct trap levels (referred to here as trap 1 and trap 2) in our samples. Their time constants were obtained from the fit.

The samples were illuminated with LEDs for increasing lengths of time, and the decay of the photoconductance was monitored for up to 10 min after the LED was terminated. This decay was then fitted with two exponentials and the amplitudes of the two exponential decays were then used to obtain the fraction of traps that are not yet filled after the given filling pulse,

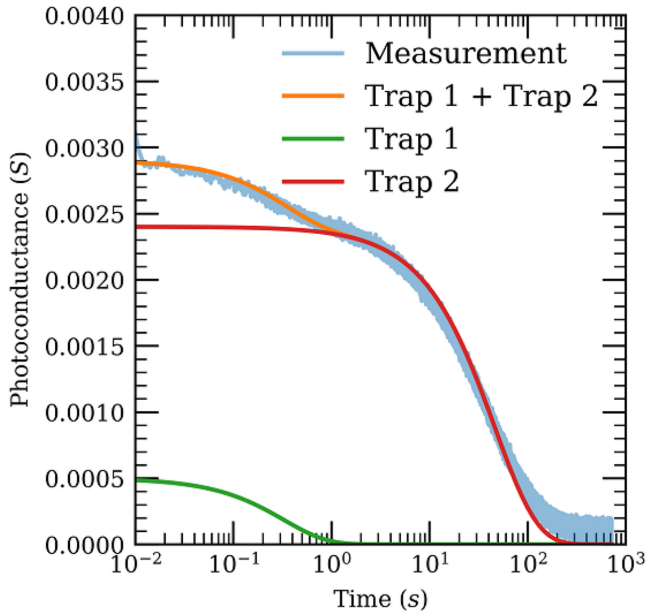

Fig. 2. Long decay of photoconductance measurements of the sample with a thermal donor concentration of 7.8×10^{15} cm^{-3} after excitation via a flash.

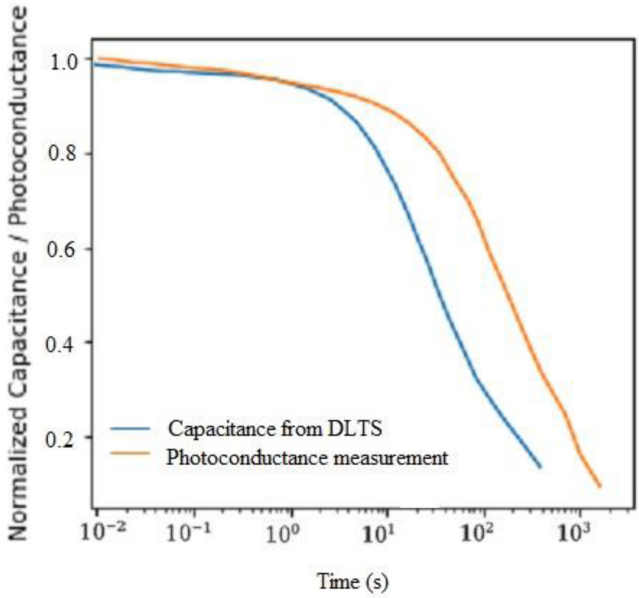

Fig. 3. Photocapacitance measurement from DLTS in [7] at the temperature of 280 K and the long decay of photoconductance measurements from this work for a sample at 278 K after excitation via a flash.

as explained previously. Here, the mobility calculations from the model of Arora *et al.* [30] using the dopant concentration and thermal donor concentration that are measured by the inductive coil are used to convert the photoconductance to the excess carrier density.

To calculate the capture cross section, the capture rate, the thermal velocity of the carriers, and the excess hole concentration during the LED filling pulse are required. These can be obtained by measuring the generation rate and minority carrier lifetime. The generation rate was determined using a calibrated reference photodiode of the LED light and the reflectance of the sample. The lifetime was measured using the PL sensor under QSS conditions, since QSSPC measurements are strongly impacted by the presence of traps [3], in contrast with QSSPL measurements that are essentially immune to this effect [3]. Once the carrier generation and lifetime are known, the excess minority carrier concentration can be obtained.

IV. Results and Discussion

Fig. 2 shows the photoconductance decay of the sample with a thermal donor concentration of 7.8×10^{15} cm^{-3} after excitation by the flash. As the traps decay at different rates over timescales of seconds, by plotting the decay curve as a function of time, we can identify two distinct traps, allowing two exponential fits, from which the decay time constant, τ_{decay}, of the two traps are estimated. The decay time constants extracted from the transient are estimated as 0.33 s for trap 1 and 46.5 s for trap 2 at the temperature of 30 °C. Hornbeck and Haynes reported photoconductance decay time constants of similar slow traps of 0.045 and 300 s [4], while Hu *et al.* [33] reported a photoconductance decay constant of 167 s. Even though thermal donors were not intentionally created in the samples investigated by these previous studies, we can still conclude that our estimated emission rates are within a similar range. In addition, the emission rates for both traps are independent of the trap occupancy by holes, p_T, neither at the beginning of the decay, nor the source of excitation or the length of the filling pulse, t_f.

Fig. 3 shows the normalized values of the photoconductance as a function of time compared with the capacitance as a function of time as measured by Markevich *et al.* [7]. In both measurements, one can observe two or more different steps in the decay, indicative of at least two different trap levels. The difference in kinetics between both samples may be due to the fact that thermal donor generation was performed at different temperatures. In our study, the samples were annealed at 450 °C for 144 h, while in [7], the samples are annealed at 350 °C for 10 h. Previous studies show that different annealing temperatures and times lead to varying thermal donor configurations. Therefore, it is possible that the samples used in [7] have a different type of thermal donor. In addition, the decay time constant of the DLTS measurement is purely due to the emission of majority carriers in the depletion region, whereas in the photoconductance measurements, the decay time constant is impacted by more than one process, as suggest by (4).

As demonstrated in Fig. 4, the fraction of captured carriers in each type of trap is measured by the amplitude of the exponential decay after different filling pulse lengths. The initial height of the photoconductance is proportional to the concentration of filled hole traps following the filling pulse. The value of the photoconductance voltage at the beginning of emission is used as a proxy for the filled trap concentration of holes after filling pulse.

Fig. 5 shows the concentration of holes in trap 1 and trap 2 as a function of the filling time for the sample with a thermal donor concentration of 7.8×10^{15} cm^{-3}. The measurements

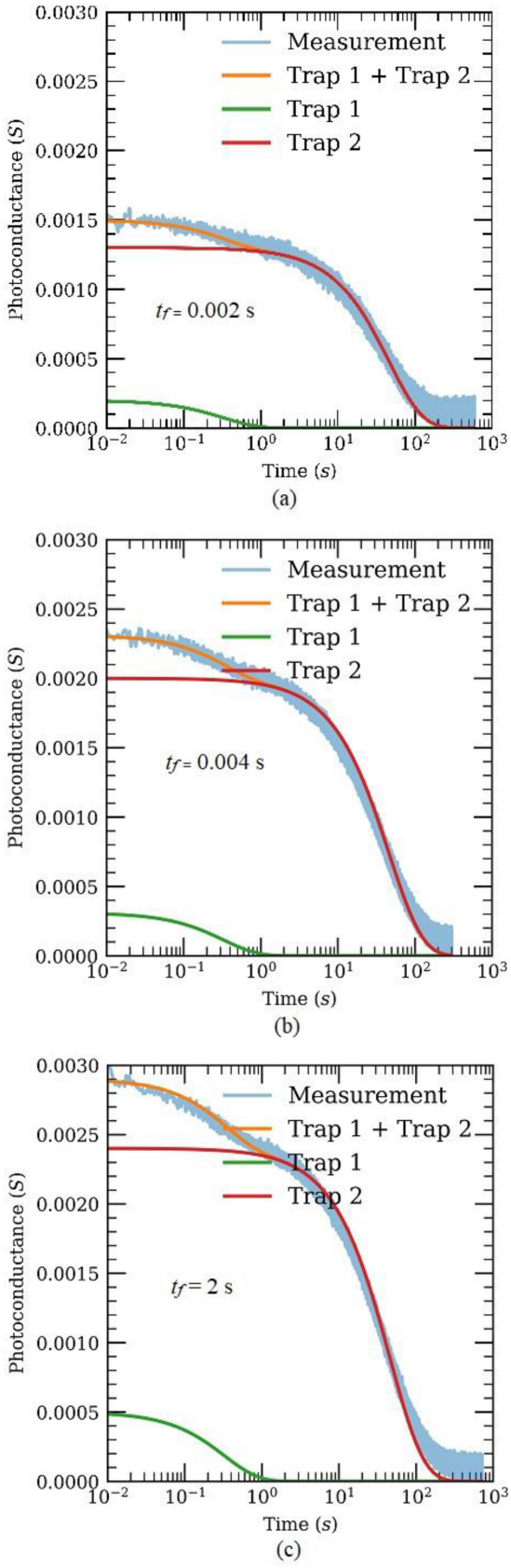

Fig. 4. Photoconductance decay measurements after an LED pulse illumination for a period (t_f): (a) 0.002 s, (b) 0.004 s, and (c) 2 s. The sample used here has a thermal donor concentration of 7.8×10^{15} cm^{-3}. The measurement temperature is 30 °C.

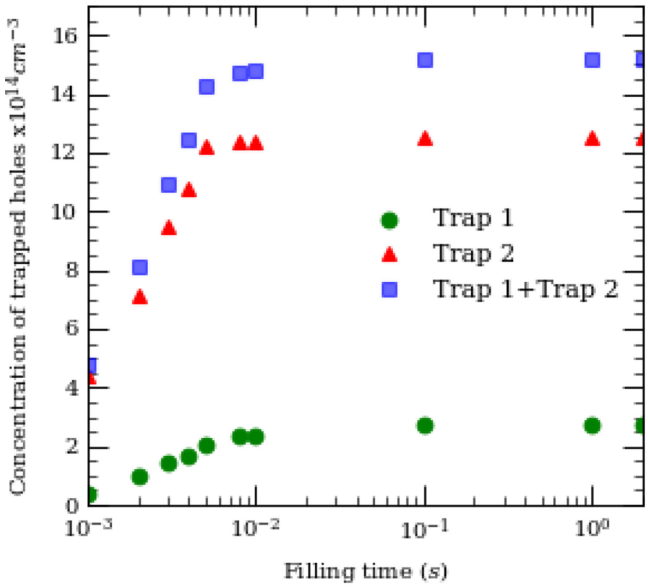

Fig. 5. Filled (hole) trap concentration after a given LED pulse light illumination for the sample with a thermal donor concentration of 7.8×10^{15} cm^{-3}at a measurement temperature of 30 °C.

TABLE I
SUMMARY OF DECAY RATE, CAPTURE RATE, AND HOLE CAPTURE CROSS SECTION OF THE SAMPLE WITH THERMAL DONOR CONCENTRATION 7.8×10^{15} CM^{-3}

Temperature	Parameter	$1/\tau_{decay}$ (s^{-1})	c_p (s^{-1})	Hole Capture Cross Section, σ_p (cm^2)
30 °C	Trap 1	3.03	245	$(3.6\pm1.2)\times10^{-18}$
	Trap 2	0.022	475	$(6.6\pm2.3)\times10^{-18}$
55 °C	Trap 1	6.67	680	$(7.2\pm2.4)\times10^{-18}$
	Trap 2	0.133	1120	$(1.5\pm0.5)\times10^{-17}$

were performed at 30 °C. These data are used to calculate the fraction of traps unfilled after each filling pulse.

As shown in Fig. 5, the occupation fractions of trap 1 and trap 2 reach a plateau for pulse lengths greater than 0.01 s. The concentration of trapped holes at 2 s is used as the steady-state trap occupancy, $p_T(\infty)$, in (4) to calculate the evolution of the trap occupancy. Fig. 6 shows the fraction of traps that are not filled by holes, $F_T(t_f)$, as a function of the pulse filling length t_f. After determining the decay rate, the capture rate is calculated by exponential fitting (see Fig. 6). Then, using the carrier generation rate by the LED illumination and the lifetime from QSSPL measurements, the respective excess carrier density and the hole capture cross section are calculated.

Table I summarizes hole capture rates (c_p), the decay rates ($1/\tau_{\text{decay}}$), and the hole capture cross sections for trap 1 and trap 2 of the sample with thermal donor concentration of 7.8×10^{15} cm^{-3}, at two different temperatures. Rougieux *et al.* [34]

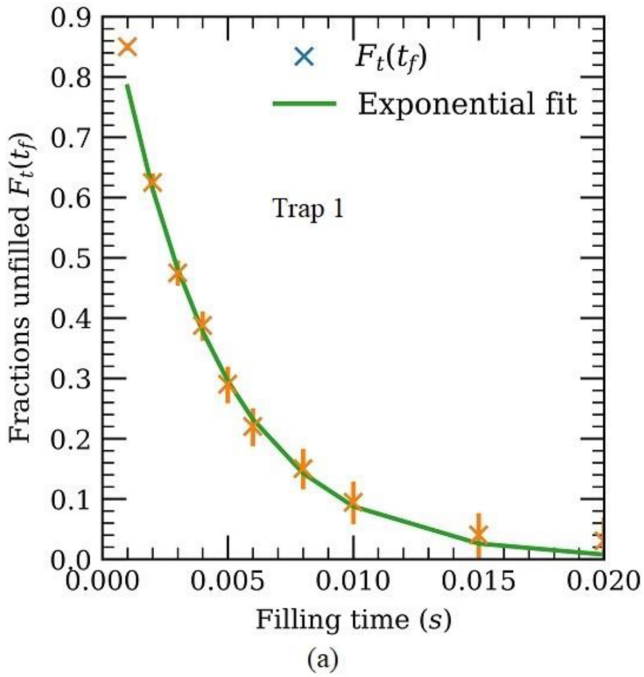

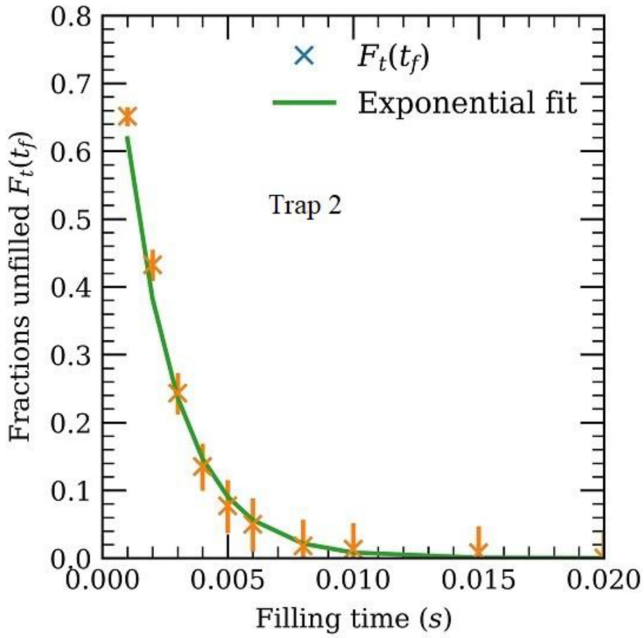

Fig. 6. Fraction of traps unfilled versus filling time at 30 °C (a) for trap 1 and (b) for trap 2 for the sample with a thermal donor concentration of 7.8×10^{15} cm^{-3}.

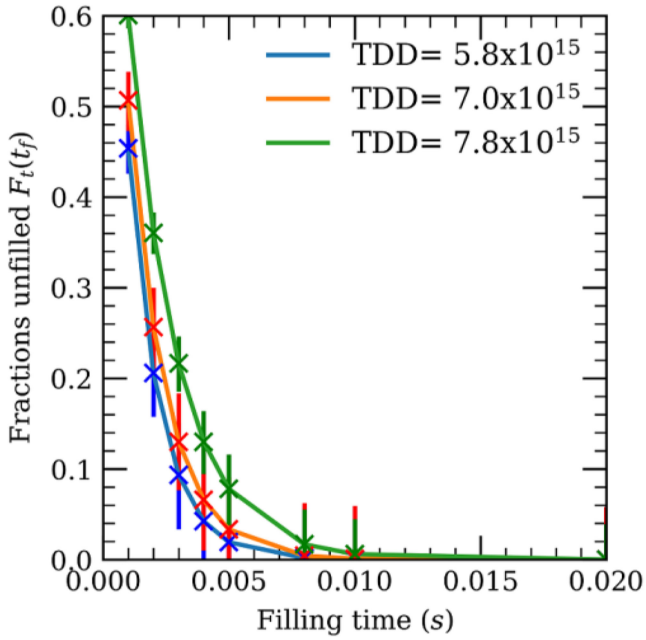

Fig. 7. Fraction of traps unfilled versus filling time at 30 °C for trap 2 for samples with different concentrations of thermal donors.

have summarized the capture cross section of different metallic defects in silicon and found that they are all within the 10^{-11} – 10^{-19} cm^2 range, while Blood [29] found that the capture cross sections of defects in GaAs are within the range of 10^{-12} – 10^{-20} cm^2. The capture cross section values estimated in this study are within the estimated values for different traps in the previous literature, although they are certainly at the low end of that range [29]. In this study, the capture cross sections for both trap 1 and trap 2 have a considerable temperature dependence. It is also observed that the capture cross section for Trap 1 has increased with temperature and that for the Trap 2 has decreased with temperature. By considering the key sources of uncertainty in the measured quantities and their propagation during the analysis, the uncertainties in the capture cross sections are estimated to be approximately 30%.

In principle, there should be no change in the capture cross section when changing the thermal donor concentration, if the defect species remains unchanged. Fig. 7 shows the fraction of empty trap 2 as a function of the pulse-filling time for samples with various thermal donor concentrations.

Table II shows the capture cross section values for the samples with different thermal donor concentrations, estimated at 30 °C, and the indicated uncertainties of 30%. The estimated values of the capture cross sections are within the uncertainty range of 30%. This may either indicate that the capture cross section values are independent of the concentration of thermal donors, or it may reflect relatively small variations due to different properties or configurations of thermal donors that are generated at different annealing periods that cannot be distinguished within the uncertainty.

As explained earlier, the emission rate is given by $\Upsilon decay = (e_p + e_n + c_n)^{-1}$. Hence, Υ_{decay} is impacted by all these three rates: c_n, e_n, and e_p. Zhu *et al.* [13] stated that the capture of electrons is essentially the recombination of an electron hole pair in the trap level and it can dominate the overall decay rate. Therefore, it is highlighted that the recombination in the trap level should not be ignored. In (4), only c_n is a function of the dopant concentration, while c_n at low injection is given by (7). Therefore, as shown in Fig. 8, by plotting $1/\Upsilon_{\mathrm{decay}}$ versus $(v_n \times n_0)$, the electron capture cross section σ_n can be estimated from the slope of the graph.

TABLE II
COMPARISON OF DECAY RATE, CAPTURE RATE, AND HOLE CAPTURE CROSS SECTION WITH TDD CONCENTRATION AT THE TEMPERATURE 30 °C

TDD concentration (cm^{-3})	Parameter	$1/\tau_{decay}$ (s^{-1})	c_p (s^{-1})	Hole Capture Cross Section, σ_p (cm^2)
5.8×10^{15}	Trap 1	2.17	440	$(1.9\pm0.6)\times10^{-18}$
	Trap 2	0.017	785	$(3.4\pm1.1)\times10^{-18}$
7.0×10^{15}	Trap 1	2.63	360	$(2.0\pm0.7)\times10^{-18}$
	Trap 2	0.019	765	$(4.3\pm1.4)\times10^{-18}$
7.8×10^{15}	Trap 1	3.03	245	$(3.6\pm1.2)\times10^{-18}$
	Trap 2	0.022	485	$(6.6\pm2.3)\times10^{-18}$

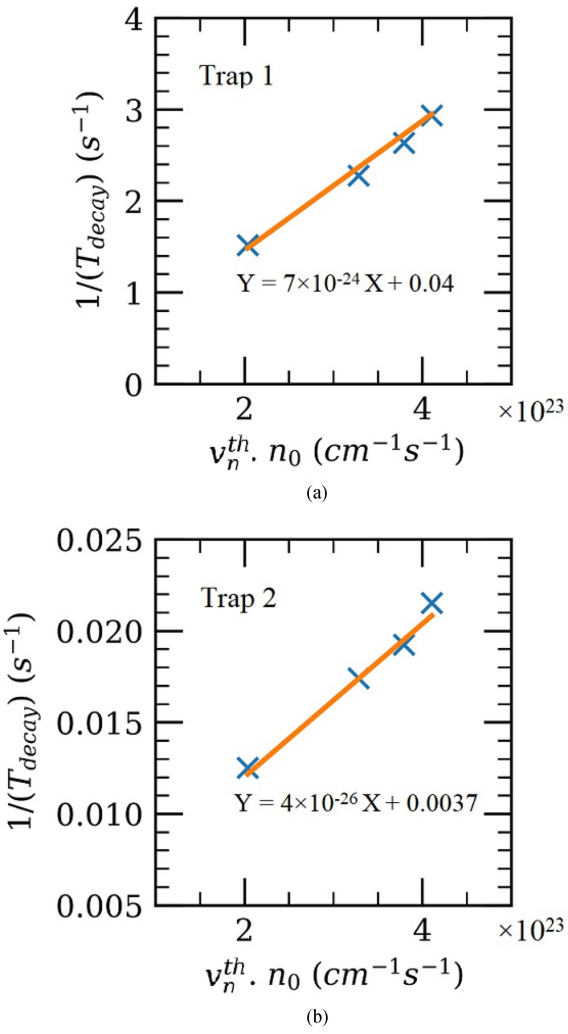

Fig. 8. Graph of $1/\tau_{\mathrm{decay}}$ versus $(v_n \times n_0)$ for the Trap 1 and the Trap 2 at 30 °C. The electron capture cross section is given by the slope and $(e_n + e_p)$ is given by the intercept of the graph.

Table III gives the summary of the estimated majority carrier (electron in this case) capture cross section data. The validity of this method in estimating the majority carrier cross section is demonstrated by Zhu *et al*. [13] in their model analysis earlier and the majority carrier capture cross section for the Trap 2 is quite similar to what Zhu *et al*. [13] have reported in their paper. The majority capture cross section values are lower than the previously recorded values in [29] and [34]. The fact that no data exist for capture cross sections below 10^{-20} cm^2 may be a reflection on the sensitivity of the tools used and the maximum length of filling pulse commonly used in capacitance transient spectroscopy, rather than a physically meaningful limit on the capture cross sections. Blood and Harris [21] report that due to constraints and limitations in the existing measuring techniques, only a fraction of the large number of different traps have been estimated.

TABLE III
ELECTRON CAPTURE CROSS SECTION OF THE SAMPLES AT 303 K

Temperature	Parameter	Electron Capture Cross Section, σ_n (cm^2)
30 °C	Trap 1	$(7\pm2)\times10^{-24}$
	Trap 2	$(4\pm1)\times10^{-26}$

The exact origin of the traps in n-type Cz silicon can be from many different sources. However, in this work, since the traps are not observed in the sample without thermal donors, the traps are believed to originate from the thermal donors. The intercept of the linear plot $1/\tau_{\mathrm{decay}}$ versus $(v_n \times n_0)$ also provides information about the trap. By solving the equation, $Intercept = \sigma_n v_n n_1(E_t) + \sigma_p v_p p_1(E_t)$, the energy level of the traps are obtained by iteration. When the energy level is in the upper half of the bandgap and at the estimated values, the aforementioned equation is satisfied. If the energy level is assumed to be in the lower half of the bandgap, the equation is not satisfied. This way, we obtain the information that both the traps are located in the upper half of the bandgap, and that E_t–E_i for the Trap 1 is determined to be 0.25 eV and that for the Trap 2 is 0.33 eV. It indicates that the two traps are located close to each other in the bandgap, and these findings coincide with the defect energy level found by Zhu *et al.* [13]. This may mean that the type of defects that we study in this research may be the same defects found in the previous study [13]. On the other hand, if the traps have more than one energy level, and if the

value for the intercept is a negative, this method cannot be used to estimate the energy levels.

We have conducted preliminary photoconductance measurements of p-type Cz-Si samples with thermal donors and observed that the shape of the photoconductance decay curve is similar to Fig. 2. These results indicate that p-type wafers with thermal donors also have two distinct traps. In principle, the same pulse-filling technique could be applied to estimate the carrier capture cross sections in p-type wafers.

V. Conclusion

In this article, a new technique to measure the hole capture cross section of slow minority carrier traps in silicon has been presented. The principal advantage of the technique was that it was contactless. The measurements can be performed at any temperature via a temperature-dependent photoconductance setup. Like MCTS, this technique has used an LED light source to change the trap occupancy with a pulsed light. Instead of the filling curve, the emission curve, which was much slower, has been used to study the kinetics of the trap filling process.

The hole capture cross section of the trap 1 induced by the presence of thermal donors in Cz silicon has been found to be 3.9×10^{-18} cm^2 $\pm$ 30% and that of the trap 2 to be 7.6×10^{-18} cm^2 $\pm$ 30% at 30 °C. The hole capture cross sections had a considerable temperature dependence. In addition, the capture cross section was unchanged within their uncertainty range with changes in the thermal donor concentration.

It has been also found that the majority carrier capture cross section was orders of magnitude lower than the minority carrier capture cross section, which in turn gave an indication that the slow traps were predominantly minority carrier traps.

The energy level for both Trap 1 and Trap 2 is located in the upper half of the bandgap and located close to each other at E_t–$E_i = 0.25$ and 0.33 eV.

References

[1] R. A. Sinton, A. Cuevas, and M. Stuckings, "Quasi-steady-state photoconductance, a new method for solar cell material and device characterization," in *Proc. 25th IEEE Photovolt. Spec. Conf.*, Washington, DC, USA, 1996, pp. 457–460.

[2] D. Macdonald and A. Cuevas, "Trapping of minority carriers in multicrystalline silicon," *Appl. Phys. Lett.*, vol. 74, no. 12, pp. 1710–1712, 1999.

[3] R. A. Bardos, T. Trupke, M. C. Schubert, and T. Roth, "Trapping artifacts in quasi-steady-state photoluminescence and photoconductance lifetime measurements on silicon wafers," *Appl. Phys. Lett.*, vol. 88, 2006, Art. no. 053504.

[4] J. A. Hornbeck and J. R. Haynes, "Trapping of minority carriers in silicon. II. n-type silicon," *Phys. Rev.*, vol. 100, no. 2, pp. 606–615, 1955.

[5] J. A. Hornbeck and J. R. Haynes, "Trapping of minority carriers in silicon. I. p-type silicon," *Phys. Rev.*, vol. 97, no. 2, pp. 311–321, 1955.

[6] F. D. Heinz, W. Warta, and M. C. Schubert, "On the benefits of counting single photoluminescence photons for the investigation of low injection lifetime and traps in silicon," *Sol. Energy Mater. Sol. Cells*, vol. 158, pp. 107–114, 2016.

[7] V. P. Markevich *et al.*, "Electron emission and capture by oxygen-related bistable thermal double donors in silicon studied with junction capacitance techniques," *J. Appl. Phys.*, vol. 124, 2018, Art. no. 225703.

[8] M. Siriwardhana *et al.*, "Temperature dependence of slow minority carrier de-trapping in czochralski silicon with high concentrations of thermal donors," in *Proc. 35th Eur. Photovolt. Sol. Energy Conf.*, Brussels, Belgium, 2018, pp. 337–341.

[9] F. D. Heinz, T. Niewelt, and M. C. Schubert, "Experimental evidence of electron capture and emission from trap levels in Cz silicon," *Phys. Status Solidi A*, vol. 214, no. 7, 2017, Art. no. 1700292.

[10] J. Schmidt, K. Bothe, and R. Hezel, "Oxygen-related minority-carrier trapping centers in p-type Czochralski silicon," *Appl. Phys. Lett.*, vol. 80, no. 23, 2002, Art. no. 4395.

[11] K. Lauer, M. Blech, A. Laades, and A. Lawerenz, "Investigation of minority carrier trapping in silicon by MWPCD measurements," in *Proc. 24th Eur. Photovolt. Sol. Energy Conf.*, Hamburg, Germany, 2009, pp. 2060–2064.

[12] N. Schuler, T. Hahn, K. Dornich, and J. R. Niklas, "Spatially resolved determination of trapping parameters in p-doped silicon by microwave detected photoconductivity," in *Proc. 25th Eur. Photovolt. Sol. Energy Conf.*, Valencia, Spain, 2010, pp. 343–346.

[13] Y. Zhu, M. K. Juhl, G. Coletti, and Z. Hameiri, "Reassessments of minority carrier traps in silicon with photoconductance decay measurements," *IEEE J. Photovolt.*, vol. 9, p. 652, 2019.

[14] D. J. Chadi, "Core structure of thermal donors in silicon," *Phys. Rev. Lett.*, vol. 77, no. 5, pp. 861–864, 1996.

[15] R. C. Newman, "Thermal donors in silicon: Oxygen centres or self-interstitial aggregates," *J. Phys. C, Solid State Phys.*, vol. 18, pp. L967–L972, 1985.

[16] J. Li *et al.*, "Effects of oxygen related thermal donors on the performance of silicon heterojunction solar cells," *Sol. Energy Mater. Sol. Cells*, vol. 179, pp. 17–21, 2018.

[17] M. Tomassini *et al.*, "Recombination activity associated with thermal donor generation in monocrystalline silicon and effect on the conversion efficiency of heterojunction solar cells," *J. Appl. Phys.*, vol. 119, 2016, Art. no. 084508.

[18] M. Ichimaru, H. Tajiri, T. Ito, and E. Arai, "Temperature dependence of carrier recombination lifetime in Si wafers," *J. Electrochem. Soc.*, vol. 145, no. 9, pp. 3265–3271, 1998.

[19] M. Siriwardhana, D. Macdonald, F. D. Heinz, and F. E. Rougieux, "Slow minority carrier trapping and de-trapping in Czochralski silicon: Influence of thermal donors and the doping density," in *Proc. 7th IEEE World Conf. Photovolt. Energy Convers.*, Waikoloa, HI, USA, 2018, pp. 3312–3314.

[20] J. A. Borsuk and R. M. Swanson, "Capture-cross-section determination by transient-current trap-filling experiments," *J. Appl. Phys.*, vol. 52, pp. 6704–66712, 1981.

[21] P. Blood and J. J. Harris, "Deep states in GaAs grown by molecular beam epitaxy," *J. Appl. Phys.*, vol. 56, pp. 993–1007, 1984.

[22] L. Dobaczewski, A. R. Peaker, and K. B. Nielsen, "Laplace-transform deep-level spectroscopy: The technique and its applications to the study of point defects in semiconductors," *J. Appl. Phys.*, vol. 96, no. 9, pp. 4689–4728, 2004.

[23] M. Pavlović, M. Jakšić, H. Zorc, and Z. Medunić, "Identification of deep trap levels from thermally stimulated current spectra of semi-insulating CdZnTe detector material," *J. Appl. Phys.*, vol. 104, 2008, Art. no. 023525.

[24] G. Kramberger, V. Cindro, I. Mandic, M. Mikuz, and M. Zavrtanik, "Determination of the effective dominant electron and hole trap in neutron-irradiated silicon detectors," *Nucl. Instrum. Methods Phys. Res. A*, vol. 516, pp. 109–115, 2004.

[25] E. Ohta and M. Sakata, "Thermal emission rates and capture cross sections of majority carriers at vanadium centers in silicon," *Solid-State Electron.*, vol. 23, pp. 759–764, 1980.

[26] C. T. Sah, L. Forbes, L. L. Rosier, and A. F. Tasch, JR., "Thermal and optical emission and capture rates and cross sections of electrons and holes at imperfection centers in semiconductors from photo and dark junction current and capacitance experiments," *Solid-State Electron.*, vol. 13, pp. 759–788, 1970.

[27] C. H. Henry, H. Kukimoto, Q. I. Miller, and F. R. Merritt, "Photocapacitance studies of the oxygen donor in GaP. II. capture cross sections," *Phys. Rev. B*, vol. 7, no. 6, pp. 2499–2507, 1973.

[28] S. D. Brotherton and J. Bicknell, "The electron capture cross section and energy level of the gold acceptor center in silicon," *J. Appl. Phys.*, vol. 49, pp. 667–670, 1978.

[29] P. Blood and J. W. Orton, *The Electrical Characterization of Semiconductors: Majority Carriers and Electron States*. New York, NY, USA, USA: Academic, 1992.

[30] N. D. Arora, J. R. Hauser, and D. J. Roulston, "Electron and Hole Mobilities in Silicon as a Function of Concentration and Temperature," *IEEE Trans. Electron Devices*, vol. ED.29, no. 2, pp. 292–295, Feb. 1982.

[31] R. A. Sinton and A. Cuevas, "Contactless determination of current-voltage characteristics and minority-carrier lifetimes in semiconductors from quasi-steady-state photoconductance data," *Appl. Phys. Lett.*, vol. 69, no. 17, pp. 2510–2512, 1996.

[32] C. Vargas *et al.*, "Recombination parameters of lifetime-limiting carrier-induced defects in multicrystalline silicon for solar cells," *Appl. Phys. Lett.*, vol. 110, 2017, Art. no. 092106.

[33] Y. Hu, H. Schøn, Ø. Nielsen, E. J. Øvrelid, and L. Arnberg, "Investigating minority carrier trapping in n-type Cz silicon by transient photoconductance measurements," *J. Appl. Phys.*, vol. 111, 2012, Art. no. 053101.

[34] F. E. Rougieux, C. Sun, and D. Macdonald, "Determining the charge states and capture mechanisms of defects in silicon through accurate recombination analyses: A review," *Sol. Energy Mater. Sol. Cells*, vol. 187, pp. 263–272, 2018.